The dynamic shear modulus and the damping ratio of deep-seabed marine silty clay

SUN Tian, CHEN Guo-xing，Zhou En-quan
(Institute of Geotechnical Engineering, Nanjing University of Technology)

ABSTRACT:
In order to study the dynamic shear modulus and the damping ratio of deep-seabed marine silty clay, cyclic triaxial tests controlled by the strain are performed on undisturbed marine silty clay which is located more than 100m depth of the Qiongzhou Strait seabed by the hollow cylinder apparatus made by GDS. Meanwhile, the effects of effective confining pressure and the plastic index on the dynamic shear modulus and the damping ratio are investigated. According to the plastic index, void ratio and effective confining pressure, an empirical formula, which is suitable for calculating the maximum dynamic shear modulus of deep-seabed silty clay, is established. It is found that, under the same conditions, the dynamic shear modulus decreased with the increasing plastic index, however, the changing rules of damping ratio are not obvious. Based on the test results, the fitting parameters for the envelope line of both dynamic shear modulus ratio versus dynamic strain curve and damping ratio versus dynamic strain curve are obtained.

Key words: deep-seabed; marine silty clay; dynamic shear modulus; damping ratio

1. INTRODUCTION

With the development and utilization of marine resources in China, there are more and more marine structures in recent years, such as drilling platform, Seabed materials storage facilities, sea-spanning bridge and submarine tunnels. The marine environment is usually complicated, which makes submarine foundation great difference from land-based foundation when it comes to dynamic response, deformation and failure mode. More attentions should be paid on the seabed instability which causes many engineering accidents such as the settlement of on-site monitoring facilities in Mississippi Delta, the sliding and inclination of platform in Bohai Sea of China, the floating of buried pipelines after windstorm. Silty clay is widely distributed in the seabed of the Qiongzhou Strait, and the proposed Qiongzhou bay sea-crossing bridge is a cross-strait construction. Nowadays, because of the lack of references on marine soil, most research focus on the marine soil locating on the seabed surface or shallow layers in Bohai, East China Sea, and Yellow Sea where natural gas and oil are distributed densely (Niu zuomin, 1986; Lv yuejun, 2003, 2008; Xiao zhiwang, 2005). As references on the marine soil in South China Sea is much less, Kong lingwei et al. (2002) directly analyze the micromechanism of Zhanjiang Sea seabed mucky soil regarding the special engineering properties including the mineral composition, physicochemical properties, bond property, pore structure characteristics except for dynamic characteristics. Up to now, there are few research results for deep marine soil, and no research on dynamic characteristics of the Qiongzhou Strait has been conducted. Cyclic triaxial tests for dynamic shear modulus ratio and the damping ratio are performed on undisturbed marine silty clay which is located more than 100m depth of the Qiongzhou Strait seabed by the hollow cylinder apparatus made by GDS in this paper, which is beneficial to understand the dynamic characteristics of the deep seabed soil.

2. TEST EQUIPMENT AND PROCEDURES.

2.1. Test Equipment

The tests are performed using a hollow cylinder apparatus (HCA) shown in Figure 1, which is

manufactured by GDS Instruments Ltd, United Kingdom. In order to conduct the dynamic triaxial test of solid cylinder specimen, the hollow copper permeable stone base of HCA is replaced by the stainless steel round plate with the same diameter which opens screw holes and pore pressure holes an "O" type rubber ring was used to partition pore pressure channel and inner pressure channel .

（a）Hollow cylinder apparatus   （b）modified base, head cover and its modification details

Figure1 Test loading system

2.2. Test Material

The tests are carried out on 14 undisturbed marine silty clay samples, which are from six exploration drilling holes distributed around seabed of the Qiongzhou strait. The depth of the sample ranged from 103.2m to over 196.0m below the seafloor. The water content of the silty clays ranges from 20.8% to 32.9%, and the plasticity index ranges from 10.2% to 16.7%. The sample characteristics and test conditions are summarized in Table 1.

Table 1 Summary of sample characteristics and test conditions

No.	Depth(m)	Consolidation stress (kPa)	Sample description	Water content(%)	Density (g/cm³)	Void ratio	Plastic limit (%)	Plastic index (%)	Liquid index
1	103.2-103.4	690	Dark grey silty clay	26.4	1.92	1.50	22.1	10.8	0.398
2	105.0-105.2	700	caesious silty clay	21.8	1.87	1.36	19.2	12.1	0.215
3	112.4-112.6	750	caesious silty clay	25.1	1.95	1.46	21.8	10.6	0.311
4	120.0-120.2	800	caesious silty clay	26.5	1.94	1.56	21.6	12.4	0.395
5	132.0-132.2	880	caesious silty clay	29.6	1.92	1.67	24.7	14.8	0.331
6	134.5-134.7	900	caesious silty clay	21.9	1.95	1.23	18.8	10.3	0.301
7	137.0-137.2	915	caesious silty clay	32.9	1.86	1.73	25.9	16.1	0.435
8	147.25-147.45	950	caesious silty clay	31.3	1.84	1.93	25.4	16.7	0.353
9	147.3~147.5	950	caesious silty clay	20.8	1.91	1.41	18.1	12.7	0.213
10	164.0~164.2	950	caesious silty clay	25.3	1.94	1.30	21.4	11.5	0.339
11	167.85~168.05	950	caesious silty clay	21.4	1.94	1.22	19.1	11.7	0.197
12	172.75~172.95	950	caesious silty clay	20.9	1.90	1.39	18.1	14.5	0.193
13	183.7~183.9	950	caesious silty clay	21.1	1.93	1.12	19.5	10.9	0.147
14	195.8~196.0	950	caesious silty clay	22.4	1.95	1.05	20.3	10.2	0.206

2.3. Test procedure
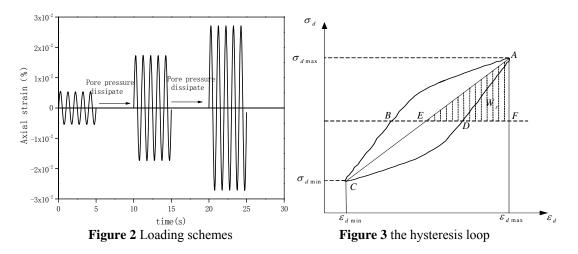
The processes of the test are as follows:
(1) according to the sample depth, the consolidation stress applied on the sample was calculated assuming the lateral pressure coefficient as 0.5, and the consolidation stress ratio as 1.0.(considering the limitation of the test equipment, the maximum consolidation pressure was 950kPa.
(2) after the preparation of the sample with the diameter of 100mm and the height of 200mm, it was placed on the hollow cylinder torsional shear apparatus.
(3) the sample was consolidated under the determined consolidation pressure
(4) after the consolidation of the sample(the criteria for judgement according to the average strain rate is less than 10^{-5}/min), the axial cyclic loading was applied on the sample step by step by increasing the strain amplitude under the undrained conditions. Each step load was cycled for five times. The load waveform is sine wave and the adopted frequency is 1Hz.
(5) record the axial load, axial strain and pore water pressure of the sample during the testing. When the pore water pressure hit 5% of the effective consolidation pressure; the sample was required for another consolidation. The next cyclic load was applied on the sample after the completion of the pore pressure dissipation.

Figure 2 Loading schemes   **Figure 3** the hysteresis loop

The elastic modulus is usually expressed as the secant modulus determined by the extreme points on the hysteresis loop, while the damping coefficient is proportional to the area inside the hysteresis loop as shown in Figure 3. It is readily apparent that each of these properties will depend on the amplitude of the strain for which the hysteresis loop is determined. Therefore, Eqs. (1) and (2) can be obtained.

$$E_d = (\sigma_{d\max} - \sigma_{d\min})/(\varepsilon_{d\max} - \varepsilon_{d\min})$$

(1)

In which σ_{dmax} and σ_{dmin} are the maximum dynamic stress and the minimum axial dynamic stress in a cycle of axial load, respectively. ε_{dmax} and ε_{dmin} are the maximum axial dynamic strain and the minimum axial dynamic strain in a cycle of axial load, respectively.

$$\lambda = W \big/ 4\pi W_s$$

(2)

In which W is the area that the hysteresis curve ABCD contained which represents the loss of energy in a cycle, and W_s is the area of the triangle AEF which is the elastic strain energy.
According to the record of the amplitude of dynamic stress and strain, the dynamic elastic modulus E_d and damping ratio λ can be calculated using Eqs. (1)and (2). According to Eqs.(3) and (4), the dynamic shear modulus G_d and damping ratio λ corresponding to dynamic shear strain amplitude γ_d can be obtained from the dynamic elastic modulus E_d and damping ratio λ

corresponding to the dynamic axial strain amplitude ε_d .

$$\gamma_d = (1+\mu_d)\varepsilon_d \tag{3}$$

$$G_d = \frac{E_d}{2(1+\mu_d)} \tag{4}$$

The value of μ_d can be obtained from Table 2.The effective consolidation pressure in the test ranges from 690kPa~950kPa The dynamic Poisson's ratio corresponding to different shear strain can be obtained as shown in Table 2, which is based on the studies of original sea soil with the effective confining pressure ranging from 700kpa and 1000kpa.

Table 2 The relationships between Poisson's ratio μ_d and generalized shear strain γ

γ （10^{-4}）	1~5	5~10	10~30	30~60	60~100	>100
μ_d	0.23	0.27	0.32	0.38	0.43	0.48

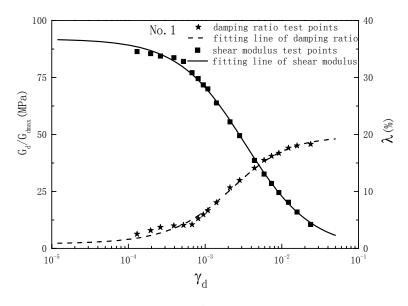## 3. RESULTS AND DISCUSSIONS

3.1. The maximum dynamic shear modulus $G_{d\max}$

The relationship between dynamic shear stress and dynamic shear strain amplitude of deep seabed silty clay can be described by a hyperbolic skeleton curve. Taking the result of No.1 for example (see Figure 4), the relation between shear-strain amplitude and secant shear modulus can be determined as:
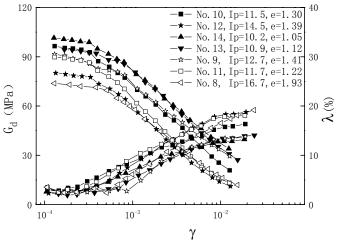
$$G_d = \frac{1}{m+n\gamma_d} \tag{5}$$

in which γ_d = shear-strain amplitude; m, n=Fitting parameters.

Figure 4 $G_d \sim \gamma_d$ 、 $\lambda \sim \gamma_d$ curves of No.1

Effective Consolidation stress is950kPa, the dynamic amplitude values of shear-strain amplitude are the same, with the increasing plastic index, the dynamic shear modulus are reduced, but changing rule of the damping ratio is not obvious as shown in Figure 5.

Figure 5 $G_d \sim \gamma_d$ 、 $\lambda \sim \gamma_d$ curves when $\sigma_0' = 950kPa$

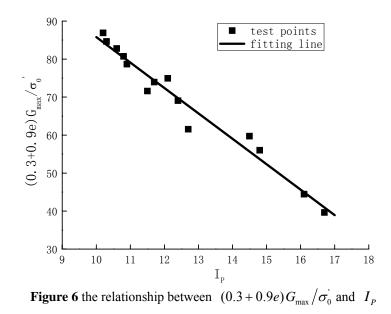Therefore, when γ_d approaches to zero, Eqs. (6) can be obtained as

$$G_{d\max} = G_d = \frac{1}{m} \tag{6}$$

The maximum dynamic shear modulus of each sample, which can be calculated by Eq. (6), are listed in Table 3.

Table 3 The maximum dynamic shear modulus (unit：MPa)

No.	1	2	3	4	5	6	7
$G_{d\max}$	91.9	79.9	100.2	94.2	88.9	107.2	75.5
No.	8	9	10	11	12	13	14
$G_{d\max}$	79.6	91.7	100.0	98.2	88.0	97.8	102.8

When the effective consolidation pressure is transformed to a dimensionless form, it is found that the dimensionless factor $(0.3+0.9e)G_{\max}/\sigma_0'$ of deep-seabed silty clay decreases linearly with the increasing plastic index as shown in Figure 6.

Figure 6 the relationship between $(0.3+0.9e)G_{\max}/\sigma_0'$ and I_P
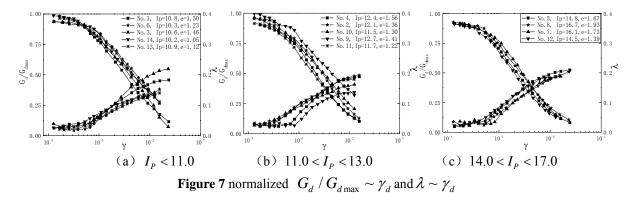
According to the test results of 38 undisturbed samples of soft marine clays from five offshore sites, Kagawa (1992) established an empirical equation to calculate the maximum dynamic shear modulus. By using the same factors including I_P, e and σ_0', an empirical formula, which is suitable for calculating the maximum dynamic shear modulus of the deep seabed silty clay, is established as follow:

$$G_{d\max} = \frac{152.7 - 6.7I_P}{0.3 + 0.9e}\sigma_0'$$

(7)

In which $\sigma_0' =$ effective confining pressure , the value of fitting parameter R^2 is 0.9620. The deep-seabed silty clay tested in this paper had water content ranging from 20.8% to 32.9%, plasticity index ranging from 10.2% to 16.7% and void ratio ranging from 1.05 to 1.93.

3.2. The modulus reduction curve $G_d / G_{d\max} \sim \gamma_d$ **and the damping ratio growth curve** $\lambda_d \sim \gamma_d$

According to the different plastic indexes, the modulus reduction curves and the damping ratio growth curves are divided into three parts as shown in Figure 7(a), (b), (c)). Figure 7 shows that when the shear-strain amplitude falls in $\gamma_d < 4\times10^{-4}$ 、 $4\times10^{-4} < \gamma_d < 1\times10^{-2}$ and $\gamma_d > 1\times10^{-2}$, the modulus reduction curves and the damping ratio growth curves have different characteristics: The former presents slow reduction, sharp reduction and slow reduction, respectively, while the later presents constant, rapid increase, and slow increase.

（a） $I_P < 11.0$　　　　　（b） $11.0 < I_P < 13.0$　　　　　（c） $14.0 < I_P < 17.0$

Figure 7 normalized $G_d / G_{d\max} \sim \gamma_d$ and $\lambda \sim \gamma_d$

The modulus reduction curve of deep-seabed silty clay can be fitted well with the empirical model,

which was proposed by Martin and Seed. Therefore, the modulus reduction curve for this model is given as:

$$\frac{G_d}{G_{d\max}} = 1 - \left[\frac{(\gamma_d/\gamma_0)^{2B}}{1+(\gamma_d/\gamma_0)^{2B}} \right]^A \tag{8}$$
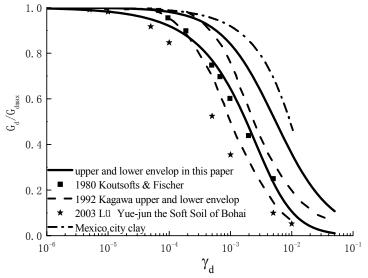
In which γ_0, A, B are fitting parameters.

The fitting values of γ_0, A, B for upper and lower envelop curve of the modulus reduction curve of deep-seabed silty clay from Qiongzhou Strait are listed in Table 4.

Table 4 The fitting values for modulus reduction model parameters

curve	$G_d/G_{d\max} \sim \gamma_d$			
parameters	$\gamma_0(\times 10^{-3})$	A	B	R^2
Upper envelop	3.48	1.544	0.481	0.9832
Lower envelop	2.52	0.688	0.585	0.9906

The reduction curves of dynamic modulus for varied clay can be seen in Figure 8 including the New Jersey cost clay tested by Koutsofts & Fischer (1980), the marine clay tested by Kagawa (1992), the Bohai Bay silty clay which is whether waxiness or hard plastic, and the Mexico City clay tested tested by Lv Yuejun (2003).The existing research results (Chen Guoxing Xie Junfei Zhang Kexu, 1995) pointed out that, void ratio (e) changed with the stress state and stress history. Void ratio and plastic index have a similar effect on the shape of the $G_d/G_{d\max} \sim \gamma_d$ curve for the same kind of cohesive soil or the clay. Meanwhile, the range for void ratio (the deep-seabed silty clay) has a smaller change. Therefore, in this paper, when analyzing the difference of the $G_d/G_{d\max} \sim \gamma_d$ curve, the influence of I_P are mainly considered. It can be seen from Figure 8 that the descent gradient of $G_d/G_{d\max}$ of the deep-seabed silty clay in Qiongzhou Strait is smaller than that of the shallow marine silty clay in the Bohai Bay, which is caused by the long depositing time of deep-seabed, also it has a large effective consolidation pressure, a good clay structure, and a slow dynamic shear modulus attenuation. Its descent gradient of $G_d/G_{d\max}$ for the deep-seabed silty clay is bigger than that of the Mexico City clay, because of its smaller value of I_P. Its reduction curve crosses with the ones tested by Kagawa, Koutsofts & Fischer, because of the similar value of I_P, in the range of 30 to 50.

Figure 8 the relationship between $G_d/G_{d\max}$ and γ_d

The relation between the shear-strain amplitude and damping ratio for the Qiongzhou Strait deep-seabed silty clay can be determined as:

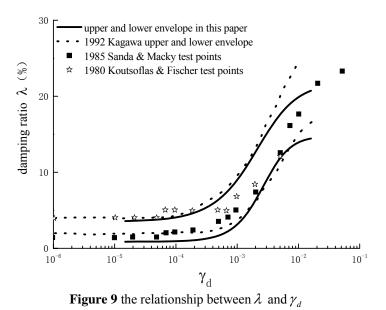$$\lambda = \lambda_p + a(1 + b\gamma^{-c})^{-d} \quad (8)$$

In which λ_p=constant, a, b, c, d are fitting parameters. The fitting values of fitting parameters in this model for upper and lower envelop curve of the damping ratio growth curve of the Qiongzhou Strait deep-seabed silty clay are listed in Table 5.

Table 5 Fitting values for damping ratio growth model parameters

curve	$\lambda \sim \gamma_d$					
parameters	λ_p	a	$b(\times 10^{-4})$	c	d	R^2
Upper envelop	3.63	17.982	1.850	-1.448	-0.75	0.9917
Lower envelop	0.86	13.921	0.068	-2.059	-0.75	0.9925

The damping ratio curves for various clays ($\lambda \sim \gamma_d$) can be seen in Figure 9 including the envelope curve of the marine clay ($\lambda \sim \gamma_d$) tested by Kagawa (1992) ,the damping ratio values for the Mexico City clay tested by Sanda & Macky (1985) ,the damping ratio values for the New Jersey cost clay tested by Koutsofts & Fischer (1980). With an increasing shearing strain, though the overall small , the trend of the damping ratio for Qiongzhou Strait deep-seabed of silty clay is similar with that for shallow seabed of silty clay when $\gamma_d \leq 1 \times 10^{-4}$, the damping ratio in the range of 0.87 to 3.63 which can be treated as a constant.

It also shows that, when $\gamma_d \geq 1 \times 10^{-2}$, the damping ratio increases more slowly than silty clay of shallow seabed, which resulted from a long deposit time, a large effective consolidation stress, a good structure and a slow increasing of damping ratio.

Figure 9 the relationship between λ and γ_d

4. CONCLUSIONS

For the first time dynamic shear modulus and the damping ratio of the Qiongzhou strait deep-seabed silty clay are studied, the main conclusions are as follows:

(1)According to the plastic index, void ratio and effective confining pressure, an empirical formula,

which is suitable for calculating the maximum dynamic shear modulus of deep-seabed silty clay, is established.

(2)With the increase of shear-strain amplitude, the modulus reduction curves and the damping ratio growth curves have different characteristics: former presents slow reduction, sharp reduction and slow reduction, respectively, while the later presents constant, rapid increase, and slow increase. Effective Consolidation stress is $\sigma^{'} = 950kPa$, the dynamic amplitude values of shear-strain amplitude are the same, with the increasing plastic index, the dynamic shear modulus are reduced, but changing rule of the damping ratio is not obvious.

(3)Based on the test results, the fitting parameters for the upper and lower envelope line of both dynamic shear modulus ratio versus dynamic strain curve and damping ratio versus dynamic strain curve are obtained.

REFERENCES

Chen Guoxing, Xie Junfei and Zhang Kexu(1995). The empirical evaluation of soil moduli and damping ratio for dynamic analysis. Earthquake Engineering and Engineering Vibration **15:1**, 73-84

Christian J T, Taylor P K, Yen J KC, et al (1974). Large diameter under water Pipeline for nuclear Power Plant designed against soil liquefaction. Proceedings of the sixth annual off-shore technology conference, Houston, Texas 597-606.

Dunlap W, Bryant W R, Williams GN, et al (1979). Storm wave effects on deltaic sediments-results of SEAWAB Ⅰand Ⅱ. Port and Ocean Engineering Under Arctic Conditions, Trondheim: Nerwegian Institute of Technology **2**, 899-920.

Gu Xiaoyun(2000). Review and prospects of marine engineering geology. Journal of engineering geology **8:l**, 40-45.

Kong Lingwei, Lu Haibo, Wang Ren and Shan Huagang(2002). Engineering properties and micro-mechanism of structural marine soil in Zhanjiang sea area. Journal of Hydraulic Engineering. **9**, 82-88

Koutsoftas, D. C, Fischer, J. A. (1980). Dynamic properties of two marine clays. Geotech. Engrg. Div., ASCE, **106:6**, 645-657.

Lv Yuejun, Tang Rongyu and Sha Haijun (2003). Experimental Study on Dynamic Shear Modulus Ratio and Damping Ratio of the Soils of Bohai Seafloor. Journal of Seismology **23:2**, 35-42.

Lv Yuejun, Peng Yanju, Shi Chunhua, Sha Haijun, , et al (2008). Study on Site Classification and Seismic Parameters for the Soft Soil of Bohai Seabed Surface Layer. rnal of Disaster Prevention and Mitigation Engineering **28:3**, 368-374.

Niu Zuomin(1986). Geotechnical characteristics and origin of absorbability of marine puddly soil in bohai gulf. Marine geology & quaternary geology **3**, 35-42.

Pan Hua, Chen Guoxing, Sun Tian (2011). Experimental research on dynamic Poisson s ratio of undisturbed marine soil. Rock and Soil Mechanics **32:s1**, 346-350.

Saada, A. S., Macky, T. A. (1985). Integrated testing and properties of a Gulf of Mexico clay. Strength testing of marine sediments: laboratory and in-situ measurements, ASTM STP 883, ASTM, Philadelphia, Pa., 363-380.

Takaaki Kagawa(1992), Moduli and Damping Factors of Soft Marine Clays. Journal of Geotechnical Engineering **118:9**,1360-1375.

Wang Shuyun; Lou Zhigang (2000). The degradation of undrained shear strength of undisturbed and remolded marine clay after cyclic loading. Rock and soil mechanics **21:1**, 20-24

Xiao Zhiwang, Yan Shuwang, Liu Run (2005). Random Field Characters of Properties of Marine Soil. Ocean Technology **24:4**, 73-79.

Zheng Jimin(1994). Marine enginering geology research in china . Journal of engineering geology **2:l**, 90-96.